Asian Journal of Geological Research

Volume 7, Issue 3, Page 232-244, 2024; Article no.AJOGER.121694

Log1DNet: A Deep Learning Architecture for Sonic Log Prediction for Seal Rock Identification in Carbon Capture and Storage Projects

Joshua Mayowa Atolagbe [a*] and Olalekan Kunle Akindele [b]

[a] Department of Geology, University of Ilorin, Nigeria.
[b] DAIM, University of Hull, United Kingdom.

Authors' contributions

This work was carried out in collaboration between both authors. Both authors read and approved the final manuscript.

Article Information

Open Peer Review History:
This journal follows the Advanced Open Peer Review policy. Identity of the Reviewers, Editor(s) and additional Reviewers, peer review comments, different versions of the manuscript, comments of the editors, etc are available here: https://www.sdiarticle5.com/review-history/121694

Original Research Article

Received: 10/06/2024
Accepted: 14/08/2024
Published: 20/08/2024

ABSTRACT

This research presents a one-dimensional Convolutional Neural Network (CNN) architecture for compressional and shear sonic logs prediction to identify potential sealing rock formation for successful carbon capture and storage (CCS) projects. Sonic logs are useful geophysical tools in the geomechanical assessment of rock layers and aid in the delineation of potential confinement and containment formations for CO_2 storage in depleted reservoirs. However, these logs are usually missing in old depleted fields due to the cost of acquisition, cycle skipping, or poor borehole condition. Therefore, a deep learning approach is proposed to predict compressional and shear sonic logs, simultaneously. Utilizing open-source data from the decommissioned Volve field in the Norwegian North Sea, Log1DNet, a fully-connected CNN model was employed to capture the trend

**Corresponding author: Email: atolagbejoshua2@gmail.com;*

Cite as: *Atolagbe, Joshua Mayowa, and Olalekan Kunle Akindele. 2024. "Log1DNet: A Deep Learning Architecture for Sonic Log Prediction for Seal Rock Identification in Carbon Capture and Storage Projects". Asian Journal of Geological Research 7 (3):232-44. https://journalajoger.com/index.php/AJOGER/article/view/167.*

of sonic log responses. A total dataset of 47,041 is gathered from five wells within the 15/9 block of the field (15/9-F-1A, 15/9-F-1B, 15/9-F-11A, 15/9-F-11T2, and 15/9-F-4). Wells 15/9-F-1A, 15/9-F-1B and 15/9-F-11A were used to train and validate the model while wells 15/9-F-11T2 and 15/9-F-4 served as the test wells, achieving an accuracy of up to 90% when compared with ground truth data. By analyzing various zonation behaviours, the detected zones were leveraged to comprehend the findings of the neural network prediction and delineate zones that can serve as a potential seal for CO_2 storage. This approach enables a faster CCS evaluation workflow characterized by low cost and high accuracy, offering significant benefits for the effective implementation of CCS initiatives.

Keywords: Sonic logs; convolutional neural network; seal; carbon storage.

1. INTRODUCTION

The presence of confinement layers (seals) is a crucial prerequisite in ensuring a sustainable CCS project [1]. Over the years, CCS themes have gained much attention in the industry. In a bid to attain net-zero emissions, various companies and research institutions have been devising strategies to reduce the concentration of CO_2 in the atmosphere by safely containing it in geologic formations. Instead of abandoning oil-depleted fields, these fields could potentially be used as carbon capture and storage sites, offering a feasible solution for geological carbon storage [2,3]. As such, impermeable seal formations are essential to facilitate the entrapment and confinement of CO_2 injected into depleted reservoirs where they are safely contained. Geophysical logs, like compressional and shear sonic logs, can be employed to identify potential seal formations.

Sonic logs are geophysical logs that measure the slowness or travel time of waves as they pass through geologic formations that a vital role in delineating targeted containment and confinement zones for CO_2 storage. However, the non-availability or missing sections of sonic logs in the old depleted fields due to the cost of log acquisition, altered zone arrivals, adverse borehole conditions or cycle skipping pose a problem. Empirical solutions using equations such as the Wyllie time average [4] and Raymer-Hunt [5] are plagued by localization problems, require unexplainable constants, and can be unreliable in uncompacted formations, limiting it to specific geologic settings. To address this, data-driven technological approaches are leveraged to generate synthetic sonic responses. This research aims to develop a deep learning methodology for predicting sonic logs to identify potential confinement formations for CO_2 storage [6].

Various traditional machine learning methods such as Genetic Algorithms Technique [7], Least Square Regression [8], Least Square Support Vector Machine [9], Random Forest and Linear Regression [10], and Gradient Boost Regressor [11], have been proposed to synthesize sonic logs. Deep learning approaches such as Artificial Neural Networks [12,13], Back Propagation Neural Networks [14], Convolutional Neural Networks and Recurrent Neural Networks [15], and Adaptive Neuro-Fuzzy Inference System [9], have also been used to generate synthetic sonic logs, achieving results greater than 80% accuracy in most cases. However, these studies synthesized either compressional logs using shear logs with acquired and/or calculated logs as input features, or combined compressional logs with acquired and/or calculated log variables to forecast shear logs. While this approach helps train the model to be more intelligent at predicting a variable, this approach may not be robust in the case of fields with limited logs. Our study considers the case of a limited log by using only the triple-combo logs such as gamma ray, resistivity, bulk density, and neutron porosity, as inputs into the proposed convolutional neural networks (CNN) architecture to predict the sonic variables, simultaneously.

This approach proved to be robust for predicting the sonic logs with high generalization strength, giving promising results when tested on new data. Subsequently, the predicted logs are interpreted to identify potential confinement zones for CO_2 storage. The use of this intelligent system approach will provide tools that facilitate elastic logs and reservoir properties prediction for faster CCS evaluation studies. Also, it will provide credible prediction results better than the empirical approach. The cost of acquiring sonic logs will be minimal, saving the company on expenditure costs, lowering computing costs, increasing computational accuracy, and removing time constrain, which will further advance the drive for net-zero policy and clean energy solutions. We highlight our main contributions in the following:

1. This work considers a limited-log scenario where only gamma ray, resistivity, bulk density, and neutron porosity logs are used to predict sonic logs.
2. We propose a one-dimensional CNN architecture called Log1DNet to predict compressional and shear sonic logs, simultaneously.
3. The network's prediction is used to identify seal formations that can potentially confine CO_2 in depleted reservoirs.

This paper is organized as follows: Section 2 discusses the geology of the study area. Section 3 presents the data and method used and the architecture of Log1DNet. Section 4 reports the performance of the model and how it was used to identify seal formations that can potentially confine CO_2.

2. GEOLOGY AND STRATIGRAPHY OF THE STUDY AREA

The data used for this study is the open-source data from the Volve field. The field is located in Block 15/9 in the southern part of the Norwegian North Sea, running at a water depth of around 80m. It lies about 200km west of Stavanger, 8km from Sleipner Ost Field, and bound to the East by Loke gas field (Fig. 1). The field was formed during the Jurassic period by the collapse of adjacent salt ridges [16]. Although, a well was initially drilled close to the crest of the structure to test the potential of the Paleocene Heimdal clastic formations, but the 4-way dip closure of the middle Jurassic Hugin Sandstone formations served as the reservoir where oil was produced. The well log data was interpreted to consist of the following stratigraphic section: the muddy sandstone of the Paleocene Heimdal formation, the Upper Cretaceous Ekofisk marl and limestone, the Upper Jurassic Draupine and Heather formations which are claystone, and the Middle Jurassic Hugin formation which is sandstone with minor clay and limestone [17]. The Callovian age Hugin sandstone formation is said to be deposited in near-shore, shallow marine environments which are interbedded by coal, claystone shale, and carbonate deposits. The trapping mechanism in the area North Sea is either stratigraphic, structural, or a combination of both. The anticline structures are highly faulted due to salt tectonics [18] and serve as primary faults that trend in the North East – South West and North West – South East directions.

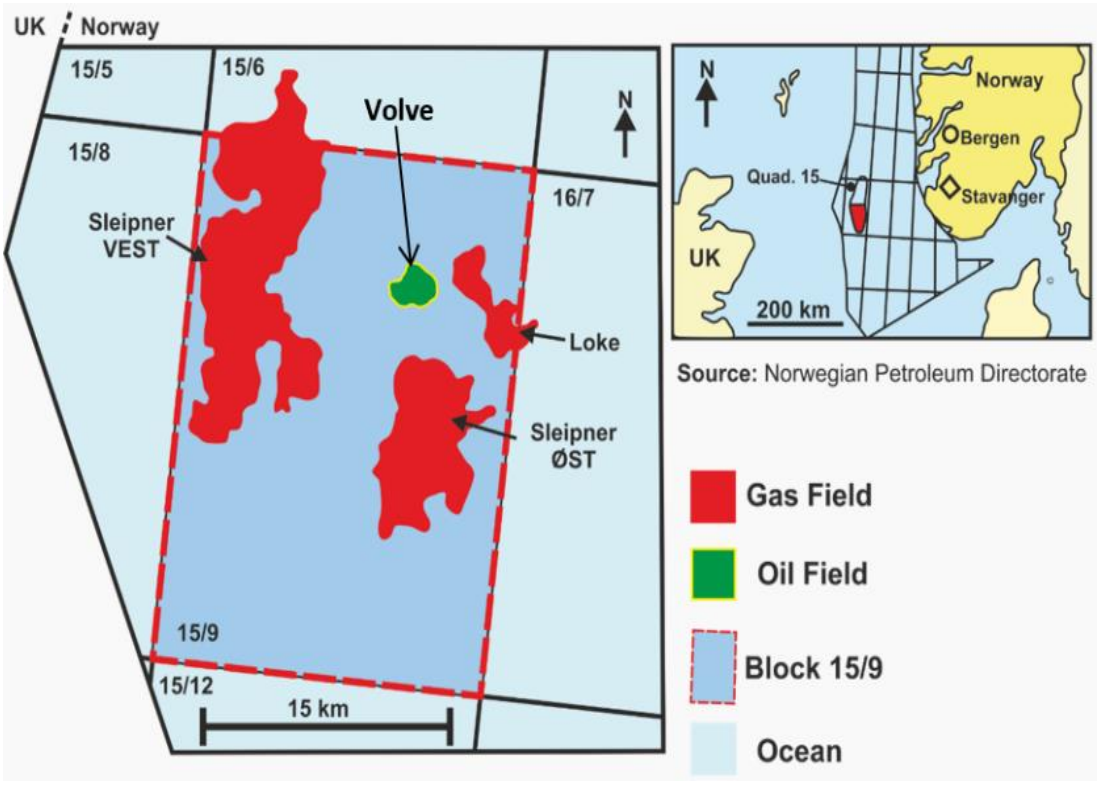

Fig. 1. Location of volve field within the block 15/9 North Sea (Wong et al. [19])

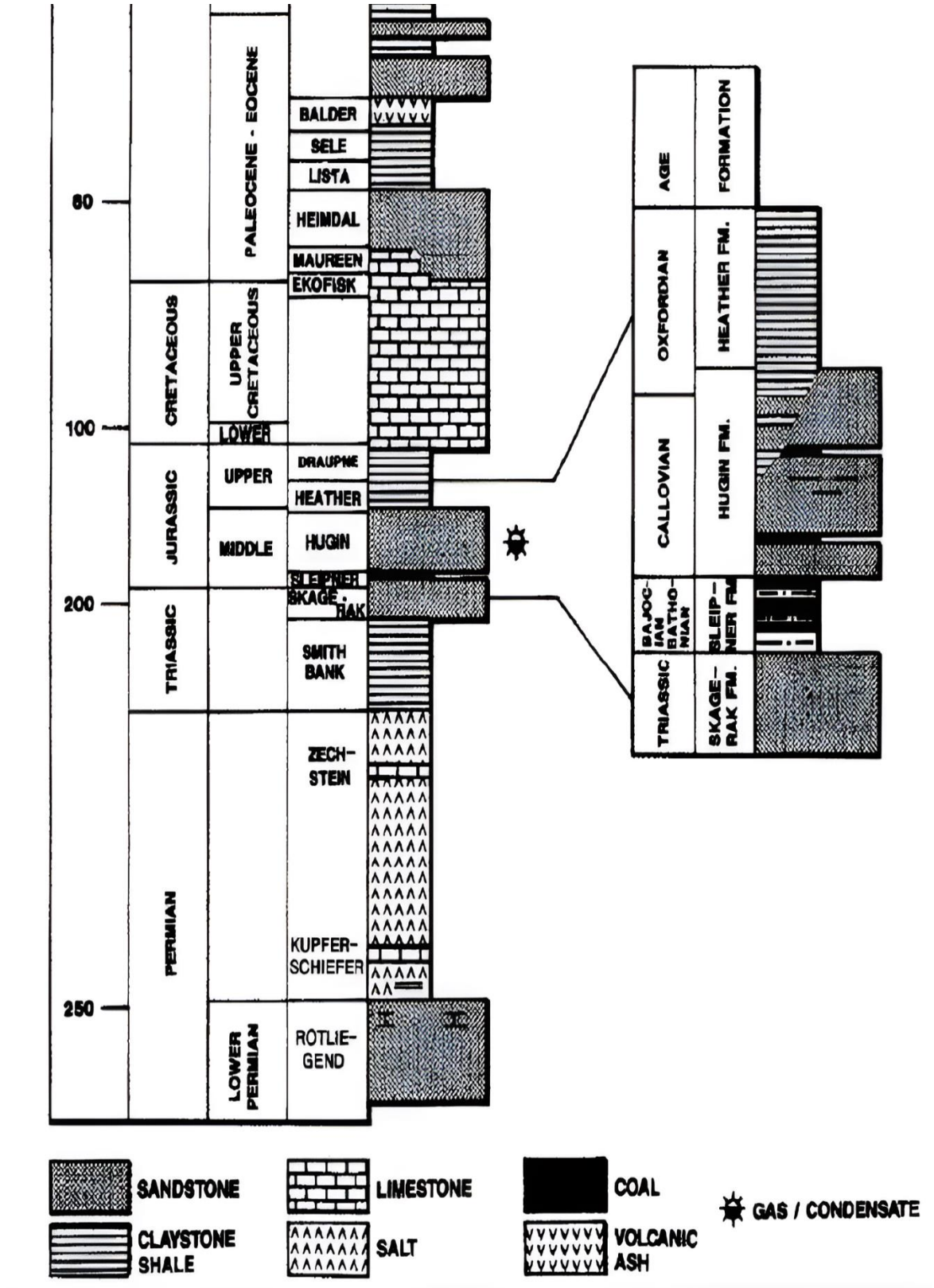

Fig. 2. A generalized stratigraphic column for the Volve field (after Al Ghaithi [15])

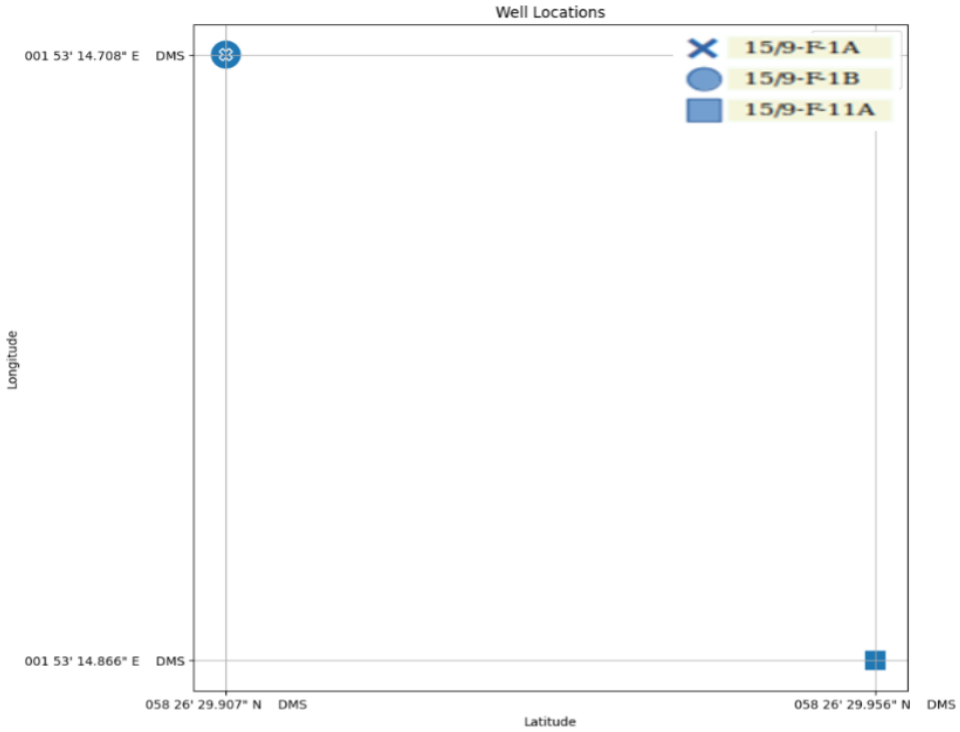

Fig. 3. Plot showing well locations

3. METHODOLOGY

3.1 Data Overview

The Volve field is characterized by a Jurassic sandstone reservoir with highly recoverable crude oil. Oil was discovered in the field in 1993, production started in 2008 and ended eight years later. To foster the research of machine learning applications in geoscience, the dataset was made available for public use in 2018, two years after production ended. This study considered only five wells within the 15/9 block, namely 15/9-F-1A, 15/9-F-1B, 15/9-F-11A, 15/9-F-11T2, and 15/9-F-4. All the wells have both DTC (Compressional) and DTS (Shear) sonic logs alongside the Gamma ray (GR), Resistivity (RT), Neutron Porosity (NPHI), and Bulk density (RHOB) logs (Table 1). The data includes measured depth ranging from about 2582.9m – 4512.9m.

Fig. 3 shows the location of the wells. This will allow the understanding of the geo-distribution of the wells and how to carefully select data for model training. Coordinate locations of three wells that are available in the original LAS file were retrieved and displayed on a base map to determine the position of the wells relative to each other. Fig. 3 shows that wells 15/9-F-1A and 15/9-F-1B were drilled close to each other, while wells 15/9-F-11A were somewhat drilled at a distance away. The data splitting process is simple. Data points from wells 15/9-F-1A, 15/9-F-1B, and 15/9-F-11A were combined, resulting in a total of 24,111 data points. Of these, 70% of the data points were randomly sampled for model training, while the remaining 30% served as a holdout set for model validation. The 22,930 data points from wells 15/9-F-11T2 and 15/9-F-4 were used to blind test the model.

3.2 Feature Selection

Feature selection is a critical step that integrates statistical validation and domain knowledge to identify and select important features for machine learning models. Statistical validation requires that the features employed for model training exhibit a strong correlation with the target variable(s). Some features have weak or negligible relationships with the target(s), therefore their statistical contribution to the modelling of an accurate predictor function will be minimal. In such cases, retaining these features as inputs into the model is not advisable.

Table 1. Training and validation wells along with theavailable well log attributes (X: means it is available)

DATA	WELL	GR	RHOB	NPHI	RT	DTC	DTS
Training	F-11A	X	X	X	X	X	X
Training	F-1A	X	X	X	X	X	X
Training	F-1B	X	X	X	X	X	X
Blind Test	F-11T2	X	X	X	X	X	X
Blind Test	F4	X	X	X	X	X	X

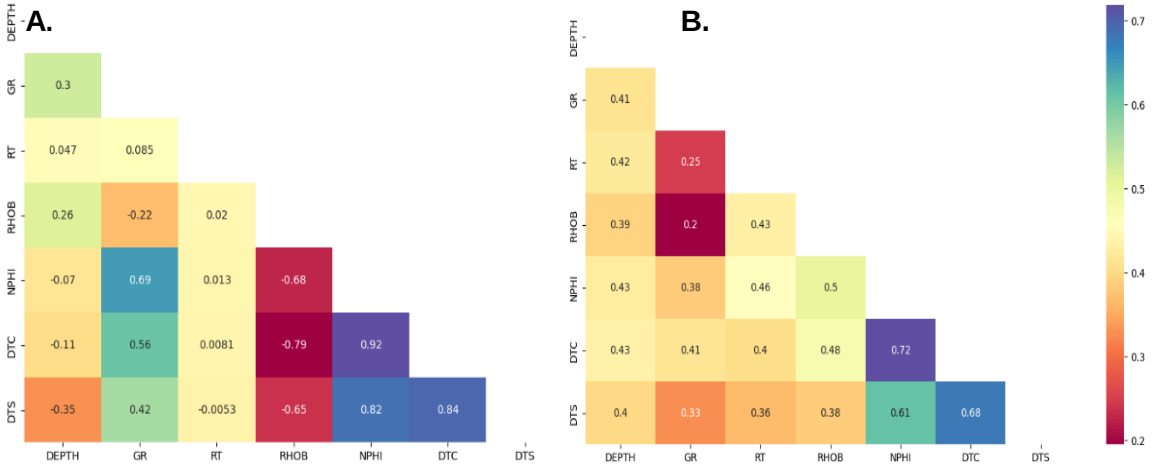

Fig. 4. Correlation heatmap (A) Chatterjee; and (B) Pearson methods of correlation between features and target of well log attributes

In this study, not all log curves in the original data will have an impact on the accurate prediction of DTC and DTS. To ascertain this, a correlation matrix between other log attributes and sonic logs was initially computed using Pearson's linear method, with RT and RHOB indicating a weak relationship with both DTC and DTS. From a domain knowledge perspective, sonic velocity is a function of how dense or compacted a formation is, while the resistivity log and the compressional sonic track each other in wet shallow clastic rocks [20]. The relationship between well attributes often exhibits non-linear patterns, and linear methods like Pearson's correlation may fail to capture these complexities [21], resulting in weak interpretations.

To validate claims based on domain knowledge and accurately capture non-linear relationships, a non-linear method such as Chatterjee correlation [22] was employed. This approach allows for a more comprehensive modelling of all input features to establish strong relationships with the sonic logs, as shown in Fig. 4. In this study, the GR, RT, NPHI, and RHOB logs were used as input features in the deep learning model.

3.3 Data Processing

This is the most important part of the workflow because, without it, models will not scale well. First, the data was processed and cleaned of missing values by dropping all the observations where at least one of the feature values was missing. Also, features such as the RT were projected from linear scale to logarithmic scale. Since RT logs are recorded as a logarithmic response, this transformation enables the model to simulate subsurface operations more accurately. Subsequently, the data were normalized to mitigate bias during training, as some features possess larger or smaller ranges than others. For instance, RT has a wide range of 0.2 to 2000 while NPHI has small value ranges of -0.15 to 0.45. The objective is to make the data attain a state of normal distribution by applying the data normalization technique, ensuring that each feature contributes equally to model training.

To achieve this, the Yeo-Johnson's Power Transformer algorithm was used to normalize the data. Power transforms are a family of parametric transformations that are applied

feature-wise to make data more Gaussian-like (bell shape) [23]. Yeo-Johnson's method supports both positive and negative data and applies unit-variance normalization to the transformed data. This normalization technique enhances the model's performance by ensuring that each feature is appropriately scaled and contributes effectively to the learning process.

3.4 Modelling

3.4.1 Architecture

Neural Networks are deep learning algorithms that simulate the processes of the human brain. The algorithm incorporates a system that contains neurons or nodes that have a collective contribution to a prediction process. A convolutional neural network (CNN) is a type of neural network used for image recognition and object detection processes and was specifically designed to process pixel data. Building a CNN architecture follows a sequential order, hence making it a suitable candidate for handling sequential data like well log data. Additionally, CNNs require very little data processing as compared to classical machine learning algorithms. However, calibrating a CNN model on two-dimensional data such as well log is feasible by reshaping the data to include an extra (third) dimension.

A typical CNN architecture starts with the input layers that accept the input features followed by kernel filters called convolutional (layers) kernels with the size that controls the length of the convolution windows. The kernel matrix convolves with the spatial input data, performs the dot product with the sub-region of the data, and gets the output as the matrix of dot products which are the feature maps. These feature maps help to detect and extract the patterns contained in each input feature. For instance, a feature map produced may detect the patterns in the RT, while another feature map contains information about the pattern found in the RHOB that will help in predicting DTC and DTS accurately. The tensor results from all these feature maps are squished and aggregated using an activation function. The non-linear Rectified Linear Unit (ReLU) activation function is a good choice to introduce non-linearity into the network and reduce errors while training the model. The result from this layer is passed into another convolutional layer or pooling layer. If passed into another convolutional layer, more feature maps will be produced, hence more pattern extraction. However, this may require higher computational power because of the increase in the size of information.

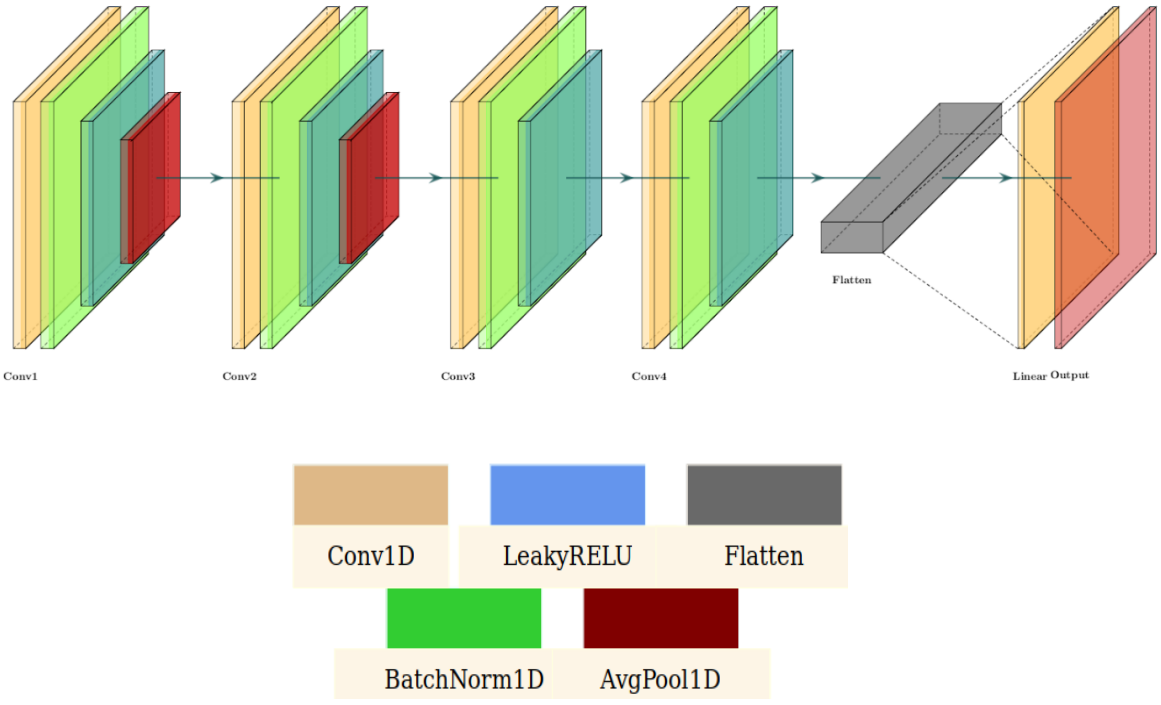

Fig. 5. The proposed Log1DNet architecture

Pooling layers usually come after a convolutional layer in a bid to reduce the spatial dimensionality of the data produced from the previous layer. It helps in decreasing the required computational power for the data processing by the method of dimensionality reduction. Its function is to extract specific information in the data by suppressing the noise in the data, therefore helping the model learn salient patterns to achieve good accuracy. The result from the pooling or convolutional layer is flattened into a vector and passed into a dense layer. While the nodes in the convolutional layers are sparsely connected, the dense layer has all its nodes connected to form a fully connected layer. At intervals between dense layers, drop-out layers may be included to control the regularization strength of the model. By regularization, the model is less prone to overfitting and able to generalize well on unseen data.

For this study, Log1DNet, a lightweight one-dimensional CNN architecture, is designed for a multi-label prediction, that is, predicts both DTC and DTS simultaneously. Fig. 5 shows the architecture of Log1DNet. It consists of four sequential 1D convolutional layers, a flatten layer, a fully connected layer and an output layer. Each convolutional layer in Log1DNet performs a one-dimensional convolution (Conv1D) to extract features from the input well log attributes (*GR, NPHI, RT and NPHI*). This is followed by batch normalization (*BatchNorm1D*) to rescale and normalize these features, enabling faster and more stable training. A non-linear activation function (*LeakyReLU*) is then applied to introduce non-linearity into the network, allowing it to learn complex patterns from the data. Finally, an average pooling layer (*AvgPool1D*) reduces the spatial dimensions of the features, helping to downsample and retain the most salient information. The number of output channels for each convolutional layer increases progressively by a factor twice the batch size. The sparse outputs from the convolutional layers are then flattened and reshaped into a one-dimensional vector (*Flatten*), which is fed into a fully connected layer (*Linear*). This layer maps the high-dimensional feature space to a lower-dimensional output space. The output layer (*Output*) has two nodes, with each node responsible for the DTC and DTS output prediction.

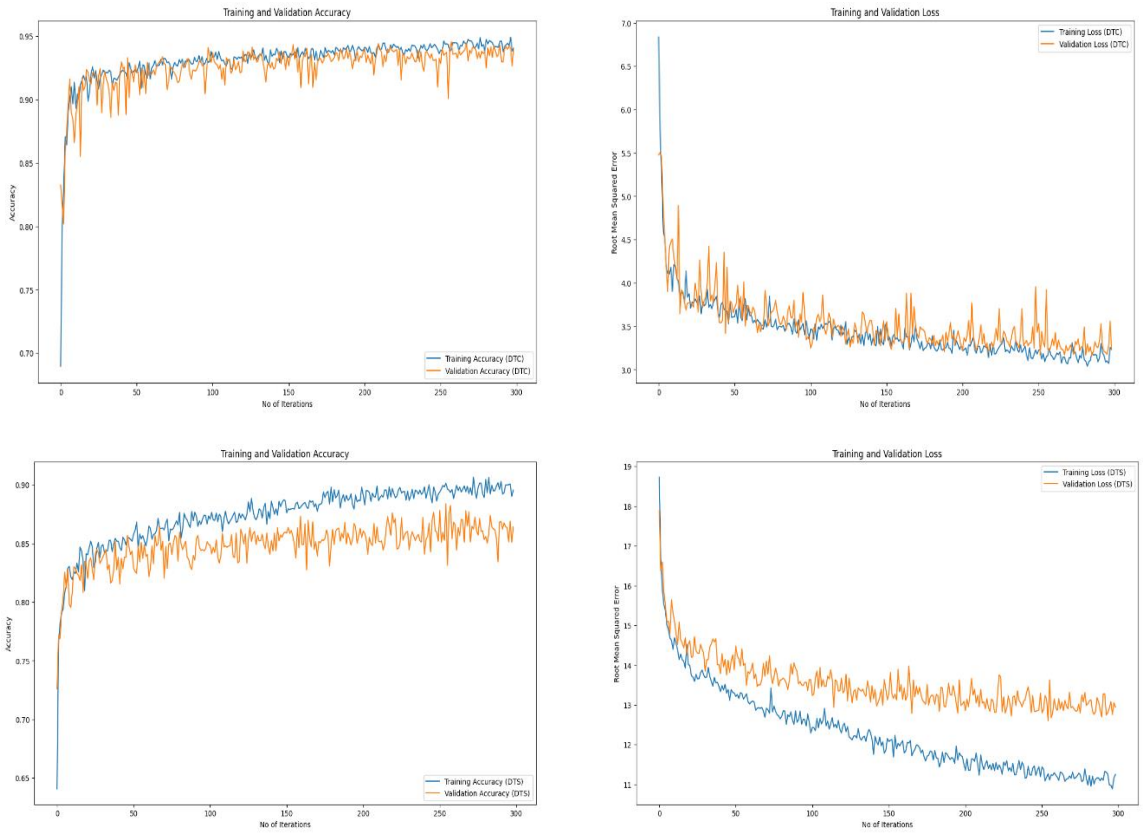

Fig. 6. Training and validation performance

3.4.2 Model training

The model was trained and tested on a Google Colab environment that offers free access to a Tesla T4 GPU with up to 16GB of memory. The model was trained over 300 epochs with a batch size of 256, using the ADAM as the optimizer. The optimizer step was controlled by introducing a small learning rate value of 1×10^{-3} and a weight decay of 1×10^{-3} to regularize the model. The parameters combined will help to adjust the model weights during the backpropagation procedure in a bid to attain optimal prediction results. It is worthy to note that the model was also tested on CPU to validate its lightweight nature.

3.5 Evaluation Metrics

The validation and error metrics used to measure the model performance include the coefficient of determination (R^2) which measures the amount of explainable variance along an axis and root mean squared error (RMSE) which measures the standard deviation of the errors a model makes in its predictions. Where *n* is the number of observations, *i* is the index number, *y* is the true value, $\hat{y}$ is the predicted value, and μ is the mean value.

$$R^2 = 1 - \frac{\sum(y_i - \hat{y}_i)^2}{\sum(y_i - \mu)^2} \qquad RMSE = \sqrt{\frac{1}{n}\sum_{i=1}^{n}(y_i - \hat{y}_i)^2}$$

4. RESULTS AND DISCUSSION

4.1 Model Results of Sonic

Analysis based on the lithology observed in the stratigraphic column (Fig. 2) revealed four distinct zones believed to have influenced the model's behavior [15]. For example, Fig. 7 shows that well 15/9-F-11A (the deepest penetrating well after 15/9-F-11T2) at about a depth of 2583m – 2792m was identified to be a sandstone or muddy sandstone interbedded with claystone, limestone, and marl was identified at 2792m – 3510m, claystone or shale sequence at 3510m – 3857m, and lastly is a clean sandstone with some clay intervals (at a measured depth greater than 3857m) which is the target reservoir [15].

The model demonstrated high precision by effectively capturing the trend of the sonic logs in comparison with the measured values. Based on the geological zones, the predictor function demonstrated accuracy in predicting both compressional and shear sonic logs across all zones, especially in the carbonate sequence. As shown in Table 2, the model achieved up to 92.7% for DTC and 77.8% for DTS in test well 15/9-F11T2. However, the prediction results for the shear log indicated discrepancies, particularly in intervals with high clay or shale content, which were both over-predicted and under-predicted. These discrepancies may arise from variations in mineral composition. Despite demonstrating an understanding of the log trends, the overall fair performance (~54% accuracy) in test well 15/9-F-4 suggests potential issues arising from these discrepancies. As such, the challenges in accurately predicting sonic logs in intervals with high clay or shale content could have contributed to the lower accuracy observed in this particular test well.

However, we believe the preprocessing workflow aided an overall improvement in the prediction results. Specifically, the logarithmic transformation of the RT log gave a spike in accuracy and low error rate as compared to using the raw values. Given that well log data are obtained from a complex and heterogeneous system, they are inherently prone to noise. Deep learning models, including CNNs, are sensitive to such noise in well log attributes. As such, we trained the model over a few epochs to mitigate the risk of overfitting by allowing the model to focus only on salient information while filtering out noise, thus facilitating good results.

Table 2. Performance of the CNN model on each well

DATA	WELL	R^2 (%)		RMSE (us/ft)	
		DTC	DTS	DTC	DTS
Training	F-11A	95.2	91.1	3.22	12.68
Training	F-1A	95.5	87.7	2.82	10.15
Training	F-1B	90.8	81.1	2.44	7.47
Blind Test	F-11T2	92.7	77.8	3.61	16.23
Blind Test	F-4	84.1	53.6	4.27	16.47

Furthermore, the training data was sampled from the shallow and deep sequence (up to 3723m), nonetheless, the model yielded a very high accuracy on testing with data points even from the deepest penetrating well (up to 4512m) that was not initially included in the training set as seen Fig. 8. This demonstrates the robustness of the model in predicting sonic logs from zones or lithologies that were not sampled as part of the training data. The model reveals a consistency in the geologic response of the retentive layers, whose results are then used to identify the potential CO_2 confinement zones based on the sonic response.

4.2 Potential Seal Formations for CO_2 Confinement

There is a direct relationship between the strength of seal rocks and sonic wave transit. The idea behind identifying a potential CO_2 confinement zone is in the degree of compaction with response to the velocity of sonic waves as they travel through formations. A denser and more compacted formation such as shale or claystone will allow a faster transit of sonic waves compared to sandstone, which is less compacted. Zones of fast travel show significant strength and are potential confinement zones, while intervals of slow travel are identified as containment zones.

In the Volve field, a potential CO_2 storage zone has been identified to be within the Hugin formation at about an average depth of 2800m – 3200m TVDSS [18]. This is justified by the increase in sonic responses and the existence of a thick shale interval that caps the saline sandstone reservoir. The properties of good sealing rocks can be inferred from their thickness, lateral extensiveness, and stratigraphic continuity. The thickness of the Viking group shale varies between 40m - 189m and extends laterally across all the study wells.

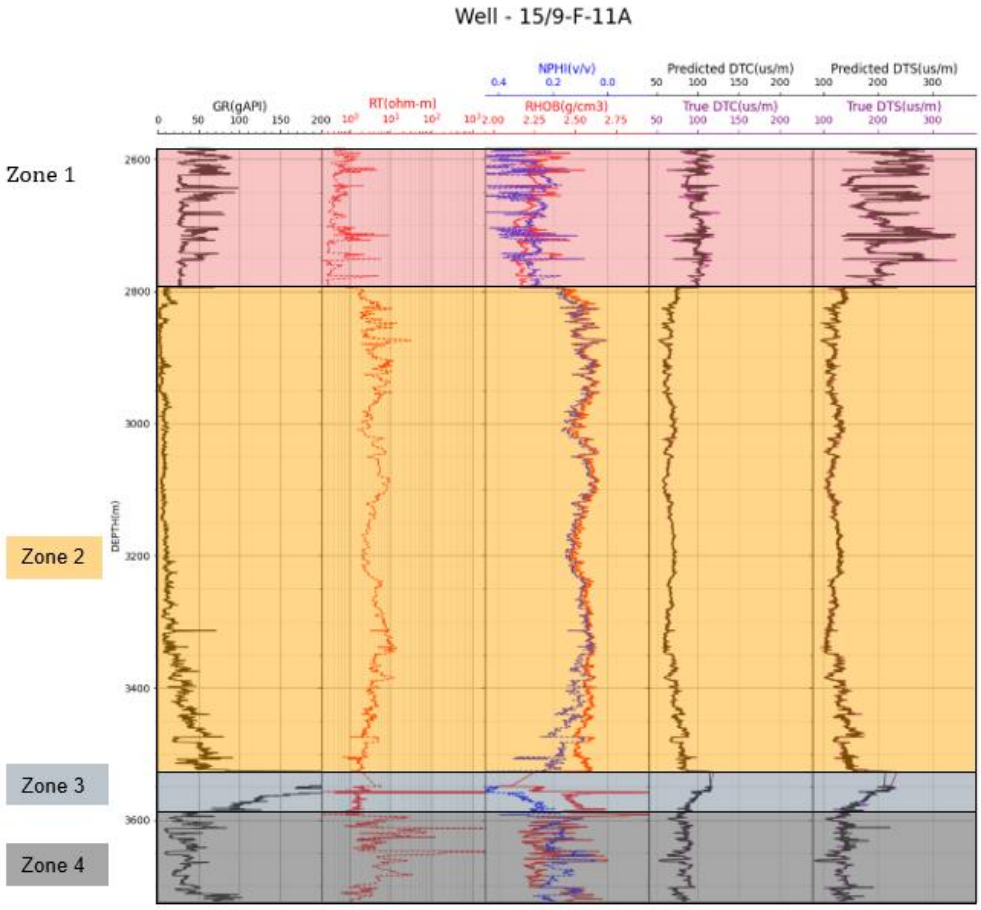

Fig. 7. Well log section showing the predicted and measured DTC and DTS in the identified zones in well 15/9-F-11A. Zone 1 is clay/muddy sandstone, Zone 2 is carbonate, Zone 3 is Shale/Claystone and Zone 4 is clean sandstone

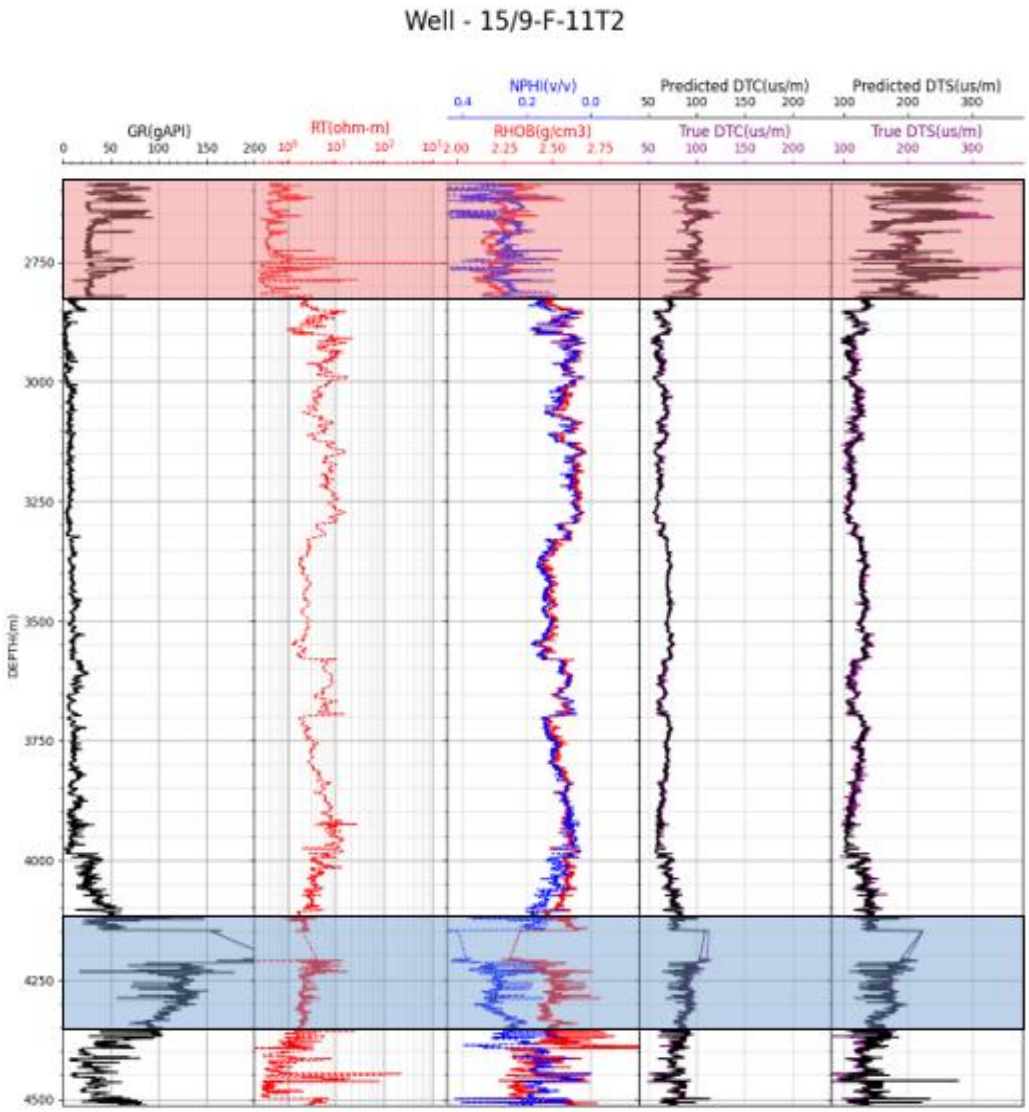

Fig. 8. Plot showing the predicted and measured DTC and DTS in test well 15/9-F11T2, along with the identified seal formations (in red and blue)

Furthermore, the major seal and storage formations exist at deeper depths, which is safe in terms of proximity to the surface. However, at a shallow depth of 2580m – 2800m, thick shale beds of the Heimdal formation (up to 40m in thickness) were also identified from the sonic response to show an overall fastness more than the deeper shale beds, indicating high confinement zones for CO2 storage.

5. CONCLUSION AND RECOMMENDATION

Previously producing oil and gas fields that have been considered uneconomical, are a prime candidate for geological sequestration with the nature of these formations able to store oil and gas over a long period. Also existing over these formations are seals that prevent further migration of fluid to the surface. This study used a deep learning approach to model a multi-label prediction of compressional and shear sonic logs to account for estimation bias by empirical methods, which was further used to identify potential seal formations for CO_2 storage in depleted reservoirs.

From the sonic interpretation, two zones were identified at shallow and deep depths to be potential retention rocks for CO_2 capture. This includes the thick claystone beds at shallow depths found in the Heimdal formation and the

thick shale of the Viking group with evidence of overall fastness in sonic transit. With this, CO_2 in the atmosphere can be reduced, leading to a sustainable future. However, the integrity of these seal formations should be further investigated through fault seal analysis. This goes beyond the scope of the current study.

DISCLAIMER (ARTIFICIAL INTELLIGENCE)

Author(s) hereby declare that NO generative AI technologies such as Large Language Models (ChatGPT, COPILOT, etc) and text-to-image generators have been used during writing or editing of manuscripts.

ACKNOWLEDGMENTS

The authors would like to thank Equinor ASA, and the Volve license partners ExxonMobil, Bayerngas Norge and Norwegian Petroleum Directorate (NPD) for the release of the Volve field data.

CODE AVAILABILITY

Codes for reproducible results are freely available here: https://github.com/joshua-atolagbe/Log1DNet

COMPETING INTERESTS

Authors have declared that no competing interests exist.

REFERENCES

1. Kaldi J, Daniel R, Tenthorey E, Michael K, Schacht U, Nicol A et al. Containment of CO_2 in CCS: Role of caprocks and faults. Energy Procedia. 2013;37:5403-5410.
Available:https://doi.org/10.1016/j.egypro.2013.06.458
2. Riis F, Halland E. CO_2 Storage Atlas of the Norwegian Continental Shelf: Methods Used to Evaluate Capacity and Maturity of the CO2 Storage Potential. Energy Procedia. 2014;63:5258-5265.
Available:https://doi.org/10.1016/j.egypro.2014.11.557
3. Ajayi T, Gomes J, Bera A. A review of CO_2 storage in geological formations emphasizing modeling, monitoring and capacity estimation approaches. Petroleum Science. 2019;16(5–6):1-36.
Available: https://doi.org/10.1007/s12182-019-0340-8
4. Wyllie MRJ, Gregory AR, Gardner, LW. Elastic wave velocities in heterogeneous and porous media. Geophysics. 1956;21(1):41-70.
5. Raymer LL, Hunt ER, Gardner JS. An improved sonic transit time-to-porosity transform. SPWLA Annual Logging Symposium. 1980;1–13.
6. Pereira P, Ribeiro C, Carneiro J. Identification and characterization of geological formations with CO_2 storage potential in Portugal. Petroleum Geoscience. 2021;27(3).
Available:https://doi.org/10.1144/petgeo2020-123
7. Moatazedian I, Rahimpour-Bonab H, Kadkhodaie-Ilkhchi A, Rajoli M. Prediction of shear and Compressional Wave Velocities from petrophysical data utilizing genetic algorithms technique: A case study in Hendijan and Abuzar fields located in Persian Gulf. Geopersia. 2011;1(1): 1-17.
Available:https://doi.org/10.22059/jgeope.2011.22161
8. He J, Misra S. Comparative Study of Shallow Learning Models for Generating Compressional and Shear Traveltime Logs. Petrophysics. 2018;59(6):826-840.
Available:https://doi.org/10.30632/pjv59n6-2018a7
9. Olayiwola T, Sanuade OA. A data-driven approach to predict compressional and shear wave velocities in reservoir rocks. Petroleum. 2021;7(2),199-208.
Available:https://doi.org/10.1016/j.petlm.2020.07.008
10. Lorentzen M, Bredesen K, Mosegaard K, Nielsen L. Estimation of Shear Sonic Logs in the Heterogeneous and Fractured Lower Cretaceous of the Danish North Sea using Supervised Learning. Geophysical Prospecting. 2022;70(8):1410-1431.
Available: https://doi.org/10.1111/1365-2478.13252
11. Tahiru I, Olagundoye O, Alabere A. Machine Learning for Sonic Logs Prediction: A Case Study from the Niger Delta Basin in the Gulf of Guinea. International Petroleum Technology Conference. 2022.
Available: https://doi.org/10.2523/iptc-21932-ms
12. Asoodeh M, Bagheripour P. Prediction of compressional, shear, and stoneley wave velocities from conventional well log data using a committee machine with intelligent

systems. Rock Mechanics and Rock Engineering. 2011;45(1):45-63.
Available: https://doi.org/10.1007/s00603-011-0181-2

13. Al Ghaithi A, Prasad M. Machine learning with artificial neural networks for shear log predictions in the Volve field Norwegian North Sea. SEG Technical Program Expanded Abstracts. 2020;450-454.
Available:https://doi.org/10.1190/segam2020-3427540.1
14. Maleki S, Moradzadeh A, Ghavami R, Gholami R, Sadeghzadeh F. Prediction of shear wave velocity using empirical correlations and artificial intelligence methods. NRIAG Journal of Astronomy and Geophysics. 2014;3(1):70–81.
Available:https://doi.org/10.1016/j.nrjag.2014.05.001
15. Al Ghaithi A. Deep Learning Methods for Shear Log Predictions in the Volve Field Norwegian North Sea. Master's thesis, Colorado School of Mines. 2020.
16. Szydlik T, Smith P, Way S, Aamodt L, Friedrich C. 3D PP/PS prestack depth migration on the Volve field. 2007;25: 43-47.
Available: https://doi.org/10.3997/2214-4609.201402177
17. Foster NH, Beaumont EA. Structural traps iv: Tectonic And Nontectonic Fold Traps, Sleipner Vest Field–Norway Southern Viking Graben, North Sea. American Association of Petroleum Geologists; 1990.
18. Sen S, Ganguli SS. Estimation of Pore Pressure and Fracture Gradient in Volve Field, Norwegian North Sea.Engineering, Geology, Environmental Science; 2019.
Available: https://doi.org/10.2118/194578-MS.
19. Wong WK, Nuwara Y, Juwono FH, Motalebi F. Sonic waves travel-time prediction: when machine learning meets geophysics. International Conference on Green Energy, Computing and Sustainable Technology. 2022;159-163.
Available:
https://doi.org/:10.1109/GECOST55694.2022.10010361.
20. Faust LY. A Velocity Function Including Lithologic Variation Geophysics. 1953;18: 271--288.
Available:https://doi.org/10.1190/1.1437869.
21. Atolagbe JM, Akinmuda OB, Okon D, Maju-Oyovwikowhe GE. Non- Parametric Machine Learning Approach to Porosity Prediction: A Case Study of an Onshore Field in Niger Delta. Nigerian Association of Petroleum Explorationists. Abstract. 2020;103
22. Chatterjee S. A new coefficient of correlation. Journal of the American Statistical Association. 2021. 2;116(536):2009-22.
Available:https://doi.org/10.1080/01621459.2020.1758115
23. Yeo I, Johnson R. A new family of power transformations to improve normality or symmetry. Biometrika. 2000;87(4):954-959.
Available:https://doi.org/10.1093/biomet/87.4.954.

Peer-review history:
The peer review history for this paper can be accessed here:
https://www.sdiarticle5.com/review-history/121694